Journal of Drug Delivery Science and Technology 79 (2023) 104052

Contents lists available at ScienceDirect

Journal of Drug Delivery Science and Technology

journal homepage: www.elsevier.com/locate/jddst

# Amlexanox-loaded nanoliposomes showing enhanced anti-inflammatory activity in cultured macrophages: A potential formulation for treatment of oral aphthous stomatitis

Afaf Abouzid [a], Abdelrhman Y. Moustafa [b,c], Natalie Allcock [d], Mohammad Najlah [e], Abdelbary Elhissi [f], Chi Wi Stanley [g], Waqar Ahmed [g,h], Peter Seville [a,i], StJohn Crean [j], Robert T. Forbes [a,**], Mohamed A. Elsawy [a,b,*]

[a] School of Pharmacy and Biomedical Sciences, University of Central Lancashire, Preston, UK
[b] Leicester School of Pharmacy, Leicester Institute for Pharmaceutical Innovation, De Montfort University, Leicester, UK
[c] Department of Industrial Pharmacy, Faculty of Pharmacy, Alexandria University, Alexandria, Egypt
[d] Electron Microscopy Facility Core Biotechnology Services, College of Life Sciences, University of Leicester, Leicester, UK
[e] Pharmaceutical Research Group, School of Allied Health, Faculty of Health, Education, Medicine and Social Care, Anglia Ruskin University, Chelmsford, UK
[f] Office of the Vice President for Research and Graduate Studies, and College of Pharmacy, QU Health, Qatar University, Qatar
[g] School of Medicine and Dentistry, University of Central Lancashire, Preston, UK
[h] School of Mathematics and Physics, University of Lincoln, Lincoln, UK
[i] School of Science and the Environment, University of Worcester, Worcester, UK
[j] Pro Vice-Chancellor Office (Research and Enterprise), University of Central Lancashire, Preston, UK

ARTICLE INFO

*Keywords:*
Amlexanox
Anti-inflammatory
Aphthous stomatitis
Liposomes
Macrophages
Oral ulcers

ABSTRACT

Oral aphthous stomatitis is a common disorder treated with the immunomodulatory drug Amlexanox (AMX), that was administered as a mucoadhesive paste (Aphthasol®). This product was discontinued by FDA in 2014 due to the associated undesired adverse reactions of the formulation. Here, we have developed AMX-loaded nanoliposome formulation as a potential alternative for the localised oromucosal delivery of AMX. Nanoliposomes were prepared using Soya phosphatidylcholine (SPC) and Cholesterol (Chol) mixtures at three different molar ratios to formulate vesicles using thin-film hydration, and were characterised for size, zeta potential and entrapment efficiency. The optimal formulation was found to be SPC:Chol 3:1 with drug entrapment efficiency of 94%, post sonication. To evaluate anti-inflammatory activity, macrophages developed by differentiation of human leukaemia monocytic cell line, THP-1, were polarised by Interferon gamma (IFNγ) and lipopolysaccharide (LPS) to M1 state. Macrophages M1 cells treated with D-L1 formulation (SPC:Chol 3:1, 500 μg/mL total lipid, and 27.6 μM AMX) showed a significant suppression in TNF-α expression levels (43 ± 2.7% of untreated control, $p < 0.05$) compared to those treated with either empty liposomes or AMX alone. Notably, % TNF-α dramatically decreased to 57 ± 4.05% of control, for cells treated with drug-free liposomes (500 μg/mL total lipid) indicating the anti-inflammatory activity of SPC lipid component per se, which led to synergistic effect as evident from the augmentation of AMX anti-inflammatory activity in D-L1 formulation. Our findings highlight the potential of using AMX nanoliposomes as a promising advanced formulation for reviving AMX treatment for management of inflammatory conditions of oral mucosa.

## 1. Introduction

Recurrent aphthous stomatitis (RAS) is a common disorder, that typically starts in childhood or adolescence. At least 1 out of 5 people can develop aphthous mouth ulcers at some stage in their life and women are affected more often than men [1]. In most cases, the individual ulcers last about 7–10 days, and ulceration episodes occur 3–6 times each year. Amlexanox (AMX) is a small molecule (molecular

* Corresponding author. Leicester School of Pharmacy, Leicester Institute for Pharmaceutical Innovation, De Montfort University, Leicester, UK.
** Corresponding author. School of Pharmacy and Biomedical Sciences , University of Central Lancashire , Preston, UK.
*E-mail addresses:* rtforbes@uclan.ac.uk (R.T. Forbes), mohamed.elsawy@dmu.ac.uk (M.A. Elsawy).

https://doi.org/10.1016/j.jddst.2022.104052
Received 15 April 2022; Received in revised form 10 November 2022; Accepted 29 November 2022
Available online 5 December 2022

weight 298.29 g/mol) poorly water soluble (146 μg/mL) lipophilic drug (logP 4.1) (Fig. 1), which is a well-established anti-inflammatory immunomodulator used to treat RAS, asthma and allergic rhinitis [2]. Topical application of AMX has been clinically verified to shorten the time for minor ulcers to heal [3].

AMX is an immunomodulatory agent that works via different mechanisms of action. It inhibits arachidonate 5-lipoxygenase enzyme preventing histamine and leukotriene release(Saijo et al., n.d.). In addition, AMX inhibits the release of S100A13 protein by blocking the heat shock protein Hsp90 [4]. S100A13 is an acidic fibroblast growth factor 1 (FGF1) implicated in a broad range of vital biological processes such as angiogenesis, cell differentiation, neurogenesis, and tumour progress. In essence, FGF1 binds to cell surface tyrosine kinase FGFRs receptors triggering cell signal transduction cascade [5]. AMX also inhibits the FGF1 release stimulating actin cytoskeleton. Thus, AMX has the ability to antagonize the angiogenic and mutagenic activity of FGF1 [5]. The most recently reported AMX mode of action is manifested by the ability of blocking the non-canonical IKK-ε and Tank Binding Kinase (IKB & TBK1). This mechanism is thought to be implicated in reduction of inflammation, reversible weight loss and improvement in insulin sensitivity [6].

The topical application of AMX is clinically very efficient in controlling RAS as it has been proven to reduce the number, size, erythema and pain associated with ulcers, as well as the significant reduction in ulceration recurrence frequency [7]. AMX was thus approved in 2004 by FDA as an anti-inflammatory treatment for oral aphthous stomatitis ulcers, in the form of a mucoadhesive paste under the name Aphthasol® [8]. Clinical trials revealed that patients topically treated with AMX 5% paste showed significant reduction in ulcer size, healing time and duration of pain compared to placebo [9]. When applied during the prodromal stage, AMX dramatically reduced the number of patients who progressed to full ulcers [9]. However, Aphthasol® was discontinued in 2014 due to the reported adverse reactions of the product, including transient pain, stinging, and burning, contact mucositis, nausea, and diarrhoea [10,11]. Therefore, there is a need for an advanced biocompatible delivery system that can enhance the selective and localised oromucosal delivery in ulcerated lesions to minimise the associated off-target side effects of AMX, for the resurrection of this effective drug. This is warranted in the absence of effective and consistent alternatives.

Liposomal drug delivery has become an established strategy for the development of such advanced delivery systems with great potential for clinical translation, thanks to the selective targeting capacity, biocompatibility and biodegradability of these lipid-based nanocarriers. A major advantage of using liposomes is the enhancement of drug cellular uptake through different postulated mechanisms, such as adsorption and fusion with phospholipid cell membranes and endocytosis [12,13]. Liposomes can protect entrapped drug molecules from metabolic enzymes and may function as a drug reservoir for controlled release [14]. Moreover, liposomal carriers have also shown to exhibit site-specific drug localisation in ulcerated areas [15,16] and instinctively target mononuclear phagocytic system, particularly macrophages, where they are naturally phagocytosed [17], thereby enhancing the therapeutic efficacy of anti-inflammatory drugs.

In light of the above, we suggested that loading AMX into liposomes formulated using naturally occurring cell membrane components (phospholipids and cholesterol), could serve as a local delivery system

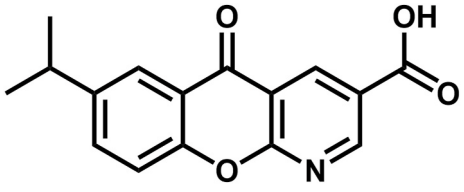


**Fig. 1.** Structural formula of the anti-inflammatory drug amlexanox (AMX).

**Table 1**
Showing treatment groups, with drug and/or lipid concentrations used.

| Treatment group | Treatment description | Drug conc. (μM) | Total lipid conc. (μg/mL)[a] |
|---|---|---|---|
| D-L1 | AMX-liposome | 27.6 | 500 |
| D1 | AMX solution | 27.6 | 0 |
| D-L2 | AMX-liposome | 13.8 | 250 |
| D2 | AMX solution | 13.8 | 0 |
| D-L3 | AMX-liposome | 2.76 | 50 |
| D3 | AMX solution | 2.76 | 0 |
| E-Lipo | Drug free liposomes | 0 | 500 |
| ASA | Acetyl Salicylic Acid solution | 27.6 | 0 |

[a] Where liposomes used, the molar ratio of SPC:Chol was 3:1.

enhancing the selective cellular uptake at the ulcerated areas of oral mucosa, augment AMX anti-inflammatory activity and minimise its adverse effects. For these reasons, we have developed AMX-loaded liposomal formulations using various soya phosphatidylcholine (SPC) to cholesterol (Chol) molar ratios, which were characterised for particle size and distribution, zeta potential and AMX entrapment efficiency. The anti-inflammatory effects were examined in pro-inflammatory macrophages M1 phenotype, which we developed by differentiation of Human leukaemia Monocytic cell line THP-1 into resting state macrophage M0, which was then polarised by interferon gamma (IFNγ) and lipopolysaccharide (LPS) into the M1 phenotype. Expression levels of the pro-inflammatory cytokine TNF-α in M1 phenotype treated with AMX, unloaded liposomes and AMX-loaded liposomes were evaluated in comparison to aspirin positive control.

## 2. Materials and methods

### 2.1. Materials

AMX (2-Amino-7-(1-methylethyl)-5-oxo-5H [1] Benzopyrano [2,3 b] pyridine-3-carboxylic acid) was purchased from Glentham Life Sciences Ltd, UK. Soya phosphatidylcholine (SPC, Lipoid S-75) was supplied by Lipoid (Steinhausen, Switzerland). Cholesterol, Bovine Serum Albumin (BSA), Dimethyl sulfoxide (DMSO) (sterile, cell culture grade), Fluorescein isothiocyanate isomer I (FITC), Lipopolysaccharides E. coli ultrapure (LPS), PBS (PH 7.2–7.4), Phenazine methosulphate (PMS), Phorbol 12-myristate 13-acetate (PMA), Tween-20 and Trypan Blue solution (0.4% w/v) were all purchased from Sigma-Aldrich, UK. Chloroform (AnalaR grade), HPLC-grade methanol, and HPLC-grade water were supplied by Fischer Scientific Ltd, UK. For cell culture, Dulbecco's Modified Eagle Medium (DMEM-500ml), L-glutamine, Non-Essential Amino Acids (NEAA) and Sodium Pyruvate were obtained from Lonza, Switzerland Foetal bovine serum (FBS) was obtained from Biosera, UK. CellTiter 96® AQueous Non-Radioactive Cell Proliferation Assay (MTS) was obtained from Promega, USA. Mounting media Vectashield® with 4′,6-diamidino-2-phenylindole (DAPI) nuclear stain was provided by Vector Laboratories, USA. Recombinant Human Interferon gamma protein (IFNγ), Substrate reagent, Human TNF-alpha DuoSet ELISA were obtained from R&D Systems Bio-Techne, UK. THP-1 cells were supplied by Leeds University (American Type Culture Collection).

### 2.2. Methods

**Preparation of liposomes.** A thin film was prepared by dissolving the soya phosphatidylcholine (M.Wt. 775 g/mol) and cholesterol (M.Wt. 386.65 g/mol) lipids at three different molar ratios (1:1, 2:1 and 3:1 mol/mol), with or without inclusion of 4 mol% AMX in a co-solvent (chloroform and methanol 2:1 v/v) to make 20 mg/mL within a round bottom flask (100 mL). The preparation solution was then evaporated under vacuum using rotary evaporator at 40 °C. A thin lipid film was formed on the inner walls of the flask, which was flushed with nitrogen

to remove any residual solvents. This was followed by hydration of the thin film with deionized water assisted with manual shaking for 10 min to form multilamellar vesicles (MLVs) (15 mg/mL). Liposomal formulations were allowed to stand for 2 h to anneal, followed by size reduction using probe-sonication. The prepared liposomes were then stored in the fridge (2–8 °C) for subsequent use. All samples were used within a maximum of 48 h after preparation.

**Size reduction of liposomes.** Probe-sonication was carried out using Sonics Vibra-cell-VC505 probe sonicator to generate nano-sized liposomes from the micro-sized multilamellar vesicles (MLVs; 10 mL, and 15 mg/mL). The probe of the sonicator was immersed in the dispersion and operated at a frequency of 20 KHz (40% amplitude) for 1 min, followed by cooling in a water bath for a few minutes to avoid overheating of the liposomes. This process was repeated until the dispersion became clear, indicating formation of nanosized liposomes, which was confirmed by size measurement via Dynamic Light Scatting (DLS) using the Zetasizer instrument (Zetasizer nano, Malvern Instruments Ltd., Malvern, UK). The resultant formulation was then centrifugated for 10 min at 10,000 rpm using Spectrafuge 24D centrifuge (Jencons-PLS, UK) to remove any leaching titanium particles from sonicator probe.

**Size analysis and zeta potential.** Measurement of size and polydispersity index (PDI) of liposomes were performed at 25 °C by DLS or Photon correlation spectroscopy (PCS) using the Zetasizer instrument (Zetasizer nano, Malvern Instruments Ltd., Malvern, UK). The zeta potential of vesicles was also determined via Laser Doppler Velocimetry (LDV) using Nano ZS after selection of the relevant software option. Prior to measurement, 100 μL of each sample was diluted with 10 mL deionized water. Measurements were carried out in triplicate using three independent preparations.

**Determination of drug entrapment efficiency.** Entrapment efficiency of AMX was determined after adapting the previously reported separation method [18–21]. The drug entrapment efficiency in sonicated and non-sonicated preparations (three batches each) were determined after separation of the unentrapped free drug from drug loaded liposomes by ultra-filtration using 0.5 mL Amicon® filters (3K Da cut-off molecular weight, (MWCO), Fisher Scientific, UK). Before ultrafiltration, the liposome preparation was centrifuged at 1000 rpm for 1 min to separate any undissolved AMX particles. Then 1 mL of supernatant was placed into the upper chamber of Amicon® centrifugal filter device, and centrifugation was conducted at 13,000 rpm for 30 min using Spectrafuge 24D, Jencons-PLS centrifuge. After centrifugation, solution of the free compounds with molecular weight less than 3 KDa passed through the filter to the bottom chamber where un-entrapped AMX was found. The AMX-loaded liposomes residue was collected from the upper chamber, where the filter membrane was placed upside down in a clean microfilter tube and centrifuged at 1000 rpm for 2 min to recover the concentrated liposomes and treated with methanol (methanol: liposomal dispersion 7:3 v/v) to disrupt the lipid layer and release the entrapped drug. Both entrapped and un-entrapped drug content were determined by HPLC (Agilent 1200 HPLC instrument, UK) equipped with UV detector ($\lambda$ 244 nm), using C-18 column (Eclipse XDB-C18, 4.6 mm × 250 mm, 5 μm, Agilent, UK) and an isocratic mobile phase of phosphate buffer solution (PH 6.5) and methanol (50:50 v/v) at a flow rate of 1.5 mL/min for 20 min. Purified liposome suspension and their respective filtrate were assessed for the encapsulation efficiency, EE%. Methanol was used to disrupt the purified liposomes and filtered using 0.45 μm syringe filter prior to HPLC measurement for quantification. The EE for AMX was calculated using equation (1):

$$EE\ (\%) = m/T \times 100 \quad (1)$$

where, m is the amount of AMX entrapped, T is the total amount of drug.

**THP-1 cell culture and macrophage differentiation.** The human monocytic leukaemia cell line, THP-1 cells (American Type Culture Collection, provided by Leeds university) were cultured in a suspension culture at 37 °C in 95% air, 5% CO2 in complete culture medium, supplemented with 10% Foetal Bovine Serum (FBS), 1 mM L-glutamine, 1 mM Sodium pyruvate and 1% non-essential amino acids. Cells were grown to a density of 1–8 × $10^5$ cells/mL and used for experiments between the passage numbers 5 and 10. The macrophage-like state was obtained by treating THP-1 cells (at a concentration of 1.5 × $10^5$ cells/mL) with phorbol 12-myristate 13-acetate (PMA, Sigma-Aldrich). PMA concentration was optimised by treating THP-1 cells with a range of PMA concentrations (3.25–200 nM) for different incubation periods (24, 48, 72 and 96 h). To assess the acquisition of a macrophage-like phenotype (cell adhesion, spreading, and increased cytoplasmic volume), cells were visualised by phase-contrast microscopy at a magnification of 400×, using a Leica inverted microscope DMIL (Leica Microsystems GmbH). Then the PMA containing culture medium was aspirated from the plates and non-adherent cells were removed by washing three times with fresh DMEM (+L-glutamine) and incubated in humidified incubator containing 5% $CO_2$ at 37 °C for additional 24 h in complete culture medium to obtain matured resting state macrophages (M0).

**Polarisation of resting state macrophages into pro-inflammatory phenotype.** The differentiated macrophages (M0) were incubated with conditioning medium (with BSA or heat inactivated serum) for 24 h, and then stimulated with fresh medium supplemented with 10 ng/mL LPS + 100 ng/mL IFNγ for 24 h. The supernatant was collected after culturing and stored at −20 °C until needed for cytokine analysis by enzyme-linked immunosorbent assay (ELISA).

**Determination of TNFα expression levels.** The TNFα concentration was measured by ELISA. After 24 h incubation with the stimulating agent (10 ng/mL LPS+100 ng/mL IFNγ), supernatant in cell cultures were collected and centrifuged at 12,000 rpm for 10 min. The production of inflammatory cytokine TNFα in the supernatant was determined using TNFα ELISA kit (R&D Systems Bio-Techne., UK). In brief, the 96-well plate was coated with 100μL/well capture antibody at 4 μg/mL, sealed with parafilm and left at room temperature for 24 h. Each well was then washed three times with Wash Buffer (PBS supplemented with 0.05% Tween-20, Sigma) and complete removal of liquid at each step was achieved by aspirating and inverting the plate and blotting it against clean paper towels. Wells were then blocked for an hour using 300 μL/well of reagent diluent (PBS supplemented with 1% BSA, Sigma.) then the washing step was repeated. Standards (15.6–1000 pg/mL) and samples were added (100 μL/well) and the plate was sealed in adhesive strip and incubated for 2 h at room temperature. The washing step was repeated before adding 100 μL/well Detection Antibody (50 ng/mL). Plates were left for 2 h before being washed and having 100 μL/well Secondary Antibody (Streptavidin -HRP) added at 1/40 dilution (50 μL Antibody + 2 mL Reagent Diluent) and left for 20 min away from light. The plates were washed, the substrate solution was added (100 μL/well) and the plates incubated for a further 20 min away from light before adding 50 μl/well of stop solution (2 N $H_2SO_4$). Plates were read at 450 nm using a plate reader (Genios Pro microtiter plate reader, Tecan, Austria). The absorbance readings for samples were used to quantify TNFα using a standard calibration curve, which was then calculated as the percentage of untreated control.

**Testing anti-inflammatory effect in macrophages.** AMX, empty liposomes, AMX-liposomes or aspirin were incubated with stimulated macrophages (M1) in order to investigate the effects of drug and carrier on modulating anti-inflammatory response of macrophages. Specifically, THP-1 cells were seeded at a density of 1.5 x$10^5$ cells/mL with PMA (25 ng/mL) in 12-well plates and differentiated at 37 °C and 5% $CO_2$ in fully humidified air for 72 h. The medium was discarded, and cells were washed with fresh DMEM (+L-glutamine) three times. Then, the cells were left in complete medium for 24 h before being polarised with 100 ng/mL IFNγ +10 ng/mL LPS for another 24 h. The treatment groups were divided into seven groups, shown in Table 1:

Additionally, cells incubated with fresh medium containing IFNγ + LPS only were used as negative control group. After being cultured

further for 24 h, the medium was harvested and the amount of TNFα was quantified by ELISA.

**Cytotoxicity assay.** Cytotoxicity was assessed using CellTiter 96 AQueous Non-Radioactive Cell Proliferation Bioassay (MTS). Briefly, 20 μL of MTS and PMS solution were added to each well of the 96 well plate and incubated for 2 h at 37 °C. The amount of soluble formazan (produced by cellular reduction of MTS) was determined by recording absorbance at 490 nm using 96-well plate reader (Tecan microtiter plate reader). The effect of varying concentrations of Amlexanox (ranging from 500 μM to 5 μM) on the viability of THP-1 differentiated macrophages was studied to validate the safety profile of the drug using MTS bioassay. Cell viability was expressed in percentage by comparing to control (n = 6). In addition, the effect of the polarising agents (IFNγ and/or LPS) was assessed using the above-described MTS protocol.

***In-vitro* cellular uptake.** To facilitate the observation of cellular uptake, the fluorescent agent Fluorescein isothiocyanate (FITC) was loaded into liposomes in an identical way to the AMX-liposomes except that the AMX was replaced for the fluorescent marker. The unloaded free FITC was removed through dialysis method (Slide-A-Lyzer, Fisher Scientific, UK). Macrophages at seeding density 1.5 x$10^5$ cells/mL were treated with various concentrations of sonicated and non-sonicated FITC-vesicles (150 μg/mL to 1.5 ng/mL), incubated for 48 h, lysed and the lysate transferred to 96-well plate and measured by GNIO pro plate reader. Fluorescence emission of the sample was quantified at 535 nm with excitation wavelength at 485 nm, each experiment had a negative control using double distilled $H_2O$ (n = 3). For confocal microscopy analysis, THP-1 cells were treated with PMA and seeded on glass-bottom dishes and incubated for 72 h. Differentiated macrophages were washed from excess PMA and left for 24 h for recovery. Different liposomes containing FITC were added and incubated for at 37 °C. Then, cells were washed with PBS three times, fixed with 4% paraformaldehyde (v/v) for 20 min, followed by cell nuclei staining with DAPI for 10 min. Cells were then viewed by a confocal laser scanning microscope (Carl Zeiss fluorescence microscopy, GmbH, Germany) and the FITC liposome fluorescence was recorded at the green channel to detect localisation in cells.

**Statistical Analysis.** All values were expressed as the mean of multiple (3–4) readings from 3 to 4 different experiments and the standard deviations (SD) were calculated. The statistical significance was assessed using the Students' t-tests for comparing two groups, and analysis of variance (ANOVA) for comparing three groups or more. The differences were considered significant when $p < 0.05$.

## 3. Results and discussion

### 3.1. Formulation and characterisation of liposomes

Liposomal formulations were prepared via thin film hydration of SPC and Chol mixtures, used at various SPC:Chol molar ratios; 1:1, 2:1 and 3:1, respectively. Probe sonication was then used to convert the generated MLVs into SUVs of approximate particle size ~100 nm as per DLS measurements (Fig. 2a) and Transmission Electron Microscopy (TEM) imaging (Supplementary Fig. S1A). Sonicated liposomes exhibited spherical morphology with no clear signs of ruptured vesicles observed in TEM, indicating that probe sonication was an effective technique for size reduction without jeopardising liposome structure integrity (Supplementary Fig. S1A). For drug loaded liposomes, AMX was incorporated in the formulations at a 4 mol% drug of total lipid mass. AMX loading did not show significant effect on liposomes size in formulations where lipid mixture of equimolar ratio was used ($p > 0.05$) (Fig. 2a). This could possibly be attributed to the compatible steric fitting of the drug molecules within the lipid bilayers of liposomes. Whereas the size of vesicles made of 2:1 and 3:1 SPC: Chol was greatly affected by AMX inclusion, where significant increase in size was observed ($p < 0.05$) (Fig. 2a), which could be due to possible interactions between AMX and SPC component of the lipid bilayer. This finding agrees with previous studies which demonstrated that inclusion of hydrophobic molecules in liposomes [22] or increasing vesicle surface hydrophobicity [23] may result in an increase of the vesicle size and polydispersity. It is possible that AMX, owing to its hydrophobicity, has increased bilayer-aqueous interfacial tension, causing increase in vesicle size.

The recorded value of polydispersity index (PDI) for drug-free liposomes was similar for all formulations ($p > 0.05$), being around ~0.46 (Fig. 2b). Strikingly, PDI values of AMX-loaded liposomal formulations revealed that vesicles generated from 3:1 SPC:Chol lipid mixture had the lowest PDI value (0.34 ± 0.04) ($p < 0.05$) (Fig. 2b). This might be a result of the more effective SPC driven drug lipid interaction in the 3:1 liposomal formulation compared to 2:1 and 1:1 liposomes of lower SPC component.

Zeta potential of all formulations were negative, because of the

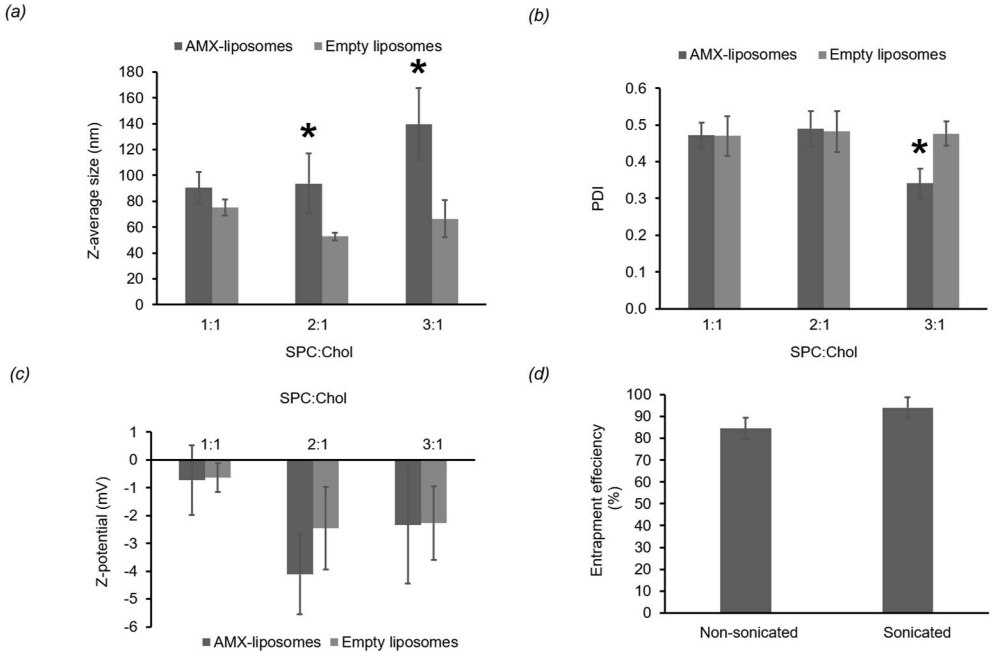


**Fig. 2. (a)** Size and **(b)** size distribution of liposomal formulations with/without AMX prepared at different molar ratios of soya phosphatidyl choline (SPC) and cholesterol (Chol). PDI: polydispersity index. **(c)** Zeta potential values of a range of liposomes before and after incorporation of AMX. **(d)** Entrapment efficiency of AMX in non-sonicated vesicles versus sonicated nanoliposomes made from SPC:Chol (3:1). Data are mean ± SD (n = 3), significantly different results (*) when $p < 0.05$.

phosphorylated SPC component (Fig. 2c). The effect of AMX loading on the liposomes surface charge was insignificant ($p > 0.05$) (Fig. 2c), implying that AMX incorporation did not compromise stability of negatively charged vesicles, where electrostatic repulsion minimised aggregation.

In order to quantify AMX entrapment in liposomes, ultra-centrifugal filtration was used to separate the un-entrapped free drug from the entrapped portion. The effect of probe-sonication on entrapment efficiency was investigated for liposomal formulation of SPC:Chol 3:1, which exhibits lowest PDI (Fig. 2b). It has been reported that the encapsulation efficiency in liposomes can be very high for water-insoluble drugs, being entrapped in the hydrophobic region between the bilayers of the phospholipid [24]. This has been observed with the lipophilic AMX (LogP 4.1), where the entrapment efficiency of non-sonicated liposomes was found to be 85%, which was further improved by sonication to reach 94% (Fig. 2d).

### 3.2. Differentiation of THP-1 to macrophages and stimulation of resting state

A pro-inflammatory cell model was developed in order to assess the anti-inflammatory effect of the liposomal formulations, where THP-1 cells were differentiated into macrophages [25,26]. Testing the effect of the differentiating agent PMA on THP-1 at a range of concentrations revealed 25 ng/mL as the lowest possible concentration causing an increase in stellate shaped cells with high adherence level to the plate, after 72 h treatment (Fig. 3a). Both change of morphology and cell attachment confirm successful differentiation of the non-adherent rounded THP-1 into adherent stellate macrophages of M0 phenotype, which became more evident 24 h after removal of the differentiating agent PMA [3,25,27–29] (Fig. 3a).

The successful transformation of resting state macrophages M0 phenotype into M1 was tested by investigating the expression levels of the pro-inflammatory factor TNFα. Resting state macrophages M0 phenotype are known to be polarised by IFNγ and LPS into the M1 state [25,30–32]. LPS is a component of the outer membrane of the Gram-negative bacteria, which is known to stimulate the secretion of many cytokines from macrophages comprising IL-1, IL-6, and TNFα [33].

As expected, resting state macrophages M0 phenotype displayed no up regulation of TNFα, and when treated with IFNγ alone, whereas an amplified TNFα expression levels were recorded after treatment with either LPS or LPS + IFNγ (Fig. 3b). These results thus confirmed the transformation of macrophages from resting state M0 to the proinflammatory phenotype M1. It is worth mentioning here that there was no significant difference in the expression levels of TNFα for cells treated with LPS and LPS + IFNγ (Fig. 3b). Though, the effect of LPS alone on reduction of cell viability was significant compared to that of IFNγ and LPS + IFNγ ($p < 0.05$) (Fig. 3c). Accordingly, herein we chose LPS + IFNγ as stimulating agent for the resting state macrophages M0 phenotype for our experiments. It has also been reported that synergistic stimulation with IFNγ and LPS is essential for the polarisation of human M1 macrophages, as opposed to stimulation with either factors alone [34–36]. It has been demonstrated that for the efficient induction of M1 phenotype in murine macrophages it required two molecular signals from the microenvironment. When macrophages were activated with IFNγ in combination with LPS, a potent tumoricidal phenotype was obtained even with the use of very low LPS concentrations [34].

Before studying the anti-inflammatory activity of AMX and liposomal formulation on THP-1 differentiated macrophages, cell viability was tested for cells treated for 24 h with a range of AMX concentrations (500 μM–5 μM). The viability was estimated to range from ~95 to 98%, indicating that free AMX did not exhibit cytotoxicity in the differentiated cell line (Fig. 3d).

### 3.3. Effect of liposomal formulation on pro-inflammatory macrophage

Our focus was to investigate the anti-inflammatory effect of pre- and post-treatment with drug-loaded liposomes (D-L1, 2 and 3), empty liposomes (E-Lipo), and drug alone (D1, 2 and 3) on the stimulated pro-inflammatory macrophage M1, where 1, 2 and 3 refer to AMX concentrations 27.6 μM, 13.8 μM and 2.76 μM, respectively. Reduction of the pro-inflammatory cytokine TNFα expression was assessed as indicator of anti-inflammatory activity, where TNFα is the principal factor

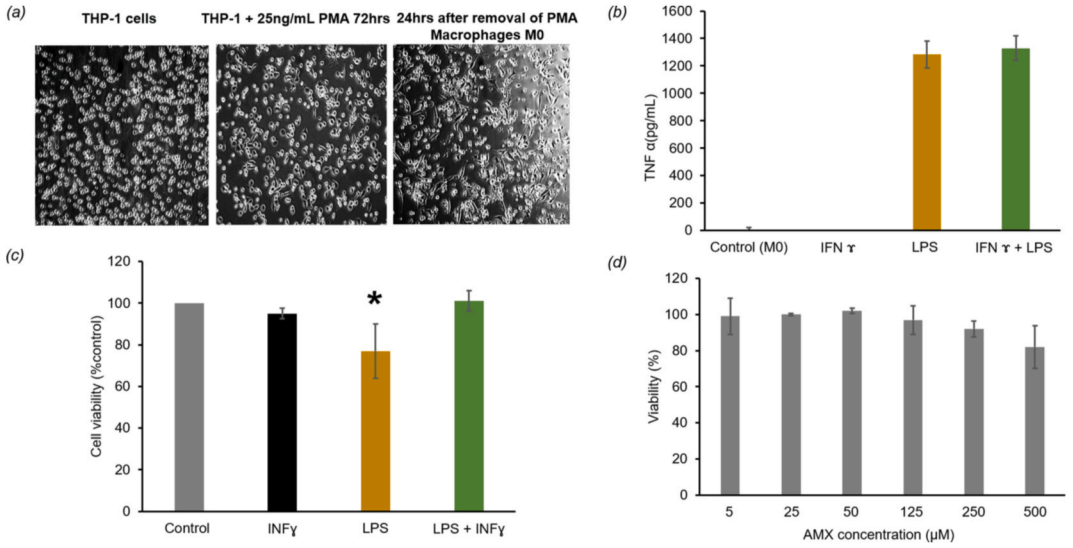


**Fig. 3.** **(a)** Optical microscope bright field images showing the difference in cell morphology and attachment tendency of the non-adherent rounded THP-1 cells before (left image) and after (middle image) incubation with the differentiating agent PMA for 72 h 24 h later, after removal of PMA and washing cell (right image), cell showed stellate morphology indicating better attachment and differentiation into the resting state macrophages (M0), original images taken at 10x magnification (scale bar 50 μm). **(b)** Effect of LPS and IFNγ on TNFα cytokine expression levels in THP-1 derived macrophages. Significant upregulation in TNFα expression was observed in cells treated with LPS and LPS + IFNγ. **(c)** Effect of LPS and IFNγ on THP-1 derived macrophages viability after 24 h of treatment. Incubation with LPS showed significant reduction of cell viability. **(d)** Cell viability of resting state macrophages M0 phenotype treated with 5–500 μM free AMX for 24 h. Results showing insignificant reduction in percentage viability compared to untreated control, across all AMX tested concentrations. Results are expressed as mean ± SD ($n = 3$), significantly different results (*) when $p < 0.05$.

regulating the secretion of inflammatory cytokine in macrophages [37] and plays a significant role in the occurrence of RAS lesions, which has been reported to increase by 2- to 5-fold in the salivary secretion of affected patients [38]. AMX is a direct inhibitor of TBK1 and IKKε, in addition, it showed to induce significant reduction of serum TNFα in mice, which is another indirect mechanism of inhibition of both kinases [6]. A comparative study was conducted for all formulations and compared to the COX-2 inhibitor aspirin (ASA) as positive control, which exhibit anti-inflammatory activity in LPS-induced macrophages through downregulation of TNFα expression via a COX2/PGE2/EP2/NF-κB pathway [39]. In addition, untreated macrophages M1 were used as negative control. Cells were incubated with the described treatments for 24 h and TNFα expression levels were assessed by ELISA.

Down-regulation of TNFα was evident post-treatment with drug-free liposomes, AMX-liposomes, free AMX, and ASA, when compared to untreated control (Fig. 4a). Dose-dependent reduction in % TNFα was not observed for cells treated with the AMX concentrations used in this study, which could be lower than that required to induce dose response. Also, this could be attributed to the little suppression of TNFα that was observed for cells treated with AMX only (reaching ~75% of untreated controls for D1, D2 and D3 treatments), due to the poor cellular uptake of the drug through passive diffusion (Fig. 4a). On the other hand, a consistent pattern of reduction in % TNFα was found in cells treated with AMX-loaded liposomal (3:1 SPC:Chol molar ratio) formulations (D-L1, D-L2 and D-L3) (Fig. 4a). For cultures treated with low concentration (D-L3) formulation (50 μg/mL nanoliposome 3:1 made from SPC to Chol molar ratio, 2.76 μM AMX content), only slight reduction in %TNFα was detected (74 ± 1.19%), which was comparable to that induced by D3 (2.76 μM AMX). By contrast, %TNFα in cells treated with D-L2 (250 μg/mL liposome, 13.8 μM drug content) was significantly lower reaching 60 ± 2.58% compared to control (Fig. 4a).

Most prominently, there was a pronounced downregulation of TNFα in macrophages treated with AMX-loaded liposomes D-L1 (500 μg/mL lipid content (3:1 SPC:Chol mole/mole), 27.6 μM AMX content), reaching 43 ± 2.72% of that expressed in the untreated control, and compared to 77 ± 6.39% in cells treated with D1 alone (27.6 μM AMX) (Fig. 4a).

Unexpectedly, ASA was found to affect TNFα levels to a limited extent, where cells treated with 27.6 μM ASA showed 83 ± 5.51% TNF expression compared to untreated control (Fig. 4a). The high potency of D-L1 formulation in supressing the pro-inflammatory cytokine TNFα, which is 3.5 folds that of ASA, suggested that there could possibly be a different mechanism by which AMX-liposomes down-regulated TNFα expression, distinct from that triggered by ASA. This hypothesis requires further mechanistic studies to understand those differences on molecular level.

Notably, %TNFα dramatically decreased to 57 ± 4.05% of control, for cells treated with the drug-free liposomes E-Lipo (500 μg/mL total lipid concentration, 3:1 SPC:Chol) (Fig. 4a). This indicates that the lipid components of the liposome possess anti-inflammatory activity per se, which led to synergistic effect as evident from the augmentation of AMX anti-inflammatory activity in D-L1 formulation (Fig. 4a). Likewise, Komalla et al. have shown that empty liposomes formed of Chol and the synthetic phospholipid 1,2-Dioleoyl-sn-glycero-3-phosphocholine (DOPC) significantly reduced IL-6 levels in TNFα stimulated primary nasal epithelial cells and suggested that the formulation can be potentially used as anti-inflammatory treatment for airway inflammation (Komalla et al., n.d.). It is also worth noting that Treede et al. reported the anti-inflammatory effect of exogenous phosphalidylcholine, which significantly reduced the production of TNFα, IL8 and other pro-inflammatory cytokines in TNFα induced Caco-2 cells [40,41]. Previous studies indicate that the anti-inflammatory mechanism of exogenous phosphatidylcholine involves suppression of LPS-induced NF-κB

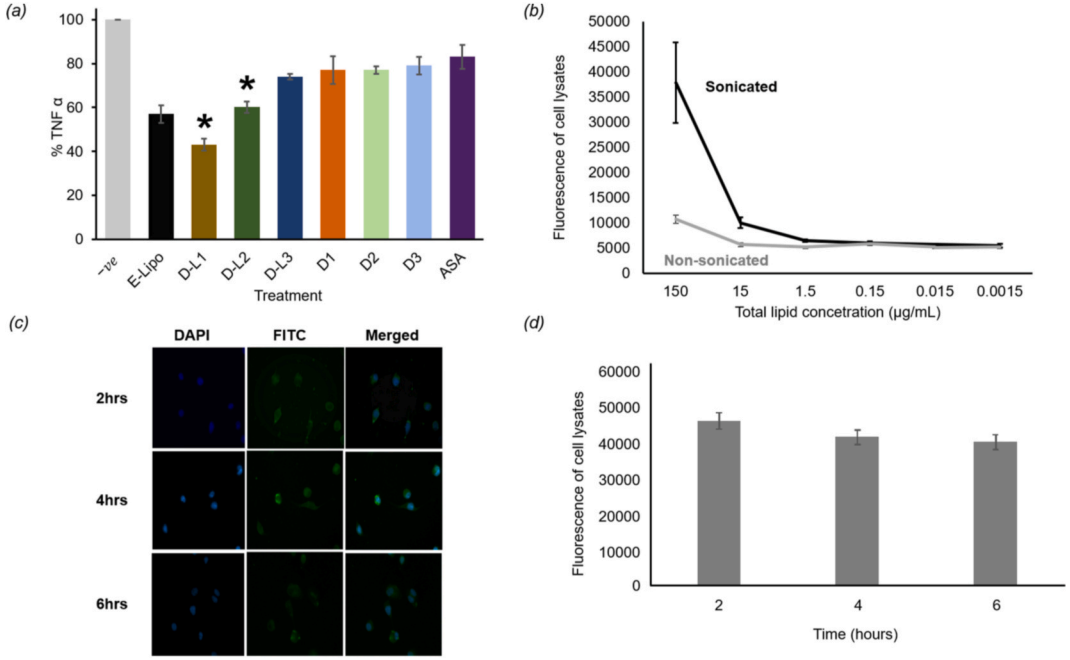


**Fig. 4.** **(a)** Percentage of TNFα expression in stimulated macrophages M1 treated with empty liposomes (E-Lipo, 500 μg/mL lipid), D-L1 (500 μg/mL lipid, 27.6 μM AMX), D-L2 (250 μg/mL lipid, 13.8 μM AMX), D-L3 (50 μg/mL lipid, 2.76 μM AMX) and aspirin (ASA, 27.6 μM) compared to untreated control. Significant reduction in % TNFα expression levels were observed in cells treated with D-L1 and D-L2 formulations. Results are expressed as mean ± SD (n = 3), significantly different results (*) when $p < 0.05$ **(b)** Fluorescence levels of macrophages M1 lysates treated with sonicated (black line) and non-sonicated (grey line) FITC-loaded liposomes (lipid concentration range 150 μg/mL to 1.5 ng/mL). Enhanced cellular uptake was achieved with sonicated formulations. To study uptake kinetics, cells were treated with FITC-loaded sonicated liposomes for 2, 4 and 6 h, where both **(c)** fluorescence microscopy images showing green fluorescence of FITC and blue DAPI stained nuclei of macrophages M1 (scale bar 50 μm) and **(d)** Fluorescence intensities of cell lysates showed insignificant differences of cellular uptake at the three timepoints. Results are expressed as mean ± SD (n = 3). (For interpretation of the references to colour in this figure legend, the reader is referred to the Web version of this article.)

activation through both inhibition of MAPK signaling pathways and nuclear translocation and phosphorylation of NF-κB p65, consequently leading to significant downregulation of TNFα [42,43]. Collectively, these results imply that the SPC component of our liposomal formulations can suppress the LPS-induced NF-κB activation leading to significant downregulation of TNFα, which augments the AMX mediated TNFα inhibition. Moreover, it is anticipated that lipid components of AMX-liposomal formulations can enhance the cellular localisation of AMX in macrophages.

Liposomal localisation in macrophages was assessed by testing cellular uptake of FITC-loaded liposomal formulations, before and after sonication at a range of total lipid concentration of 150 μg/mL to 1.5 ng/mL (3:1 ratio of SPC:Chol mole/mole), to study the effect of liposomal size and lipid content on the uptake efficiency. In general, there has been a lipid concentration dependent enhancement of cellular uptake, as observed from the gradual increase in FITC fluorescence intensity of macrophage cell lysates as a function of increasing lipid concentration, for both sonicated and non-sonicated formulations (Fig. 4b). This was more obvious in sonicated nano-sized formulations (126 nm), which have been taken up by macrophages ~3 times more than the non-sonicated micro-sized vesicles (26 μm) at same lipid concentration (150 μg/mL) (Fig. 4b). These findings agree with the previously reported inverse relationship between liposome size and their in vitro uptake by bone-marrow macrophages [44]. Cellular uptake of sonicated 4% molar ratio FITC-loaded in liposomes made of 3:1 SPC:Chol was confirmed by fluorescence microscopy, which showed densely dispersed liposomes (green fluorescence) around the DAPI stained nuclei (blue fluorescence) at all the examined time points (2, 6 and 4 h), indicating the successful intracellular localisation (Fig. 4c). Fluorescence data for cell lysates showed no significant differences at the three timepoints, implying the efficient cellular uptake of the nanoliposomes within 2 h of treatment (Fig. 4d). Furthermore, stability testing of FITC-loaded liposomes in artificial saliva was performed at 37 °C revealed good stability over the 2 h period, with negligible FITC release detected during the first hour and <30% release during the second hour, indicating liposome structural integrity in a physiologically simulated environment (Supplementary Fig. S1B).

Collectively, our results showed that D-L1 formulation successfully enhanced the anti-inflammatory activity of AMX when tested in macrophages and the lipid content augmented this activity. Additionally, sonicated nanosized SPC Chol liposomes showed efficient cellular uptake by macrophages M1, thus enhancing cargo localisation, which was in a lipid concentration dependent fashion.

## 4. Conclusions

In this study, we demonstrated the potential of using AMX-loaded nanoliposomes for the efficient targeting of macrophages and modulating their inflammatory responses. Macrophages showed dose-responsive reduction in TNFα expression with increasing AMX-liposome concentration. The combination of AMX and SPC:Chol nanoliposomes (D-L1 formulation) exhibited significantly stronger anti-inflammatory effect than that of either AMX alone or empty liposomes (E-Lipo), suggesting that the used lipids augment the anti-inflammatory activity of AMX. This was confirmed by the remarkable reduction in TNFα expression in cells treated with E-Lipo. Based on previously reported studies, it can be anticipated that the SPC component of liposomal formulations has suppressed the LPS-induced NF-κB activation leading to observed significant downregulation of TNFα, thus augmenting the AMX mediated TNFα inhibition [42,43,45]. In addition, considerable cellular uptake of FITC-loaded nanoliposomes was achieved within 2 h of treatment, implying possibility of further enhancement of AMX anti-inflammatory activity through better drug localisation in target cells. Further mechanistic studies on the interaction of E-Lipo and AMX-loaded nanoliposomes with LPS-induced macrophages and the consequent intracellular signalling cascade are required to gain a deeper insight of the anti-inflammatory activity of this system. In addition, developing AMX-loaded nanoliposome formulation in mucoadhesive vehicles will be considered in future for the localised administration in buccal cavity, though in vivo validation studies using an appropriate animal model.

## Author contributions

Conceptualization, A.A., A.E., C.W.S., W.A., P.S., S.C., M.A.E. and R.T.F.; methodology, A.A., A.E., A.Y.M., C.W.S., P.S., M.A.E., N.A. and R.T.F.; formal analysis, A.A., A.Y.M. and N.A.; data curation, A.A., A.Y.M. and N.A.; writing—original draft preparation, A.A., A.Y.M., M.N., A.E., M.A.E. and R.T.F.; writing—review and editing, A.A., A.Y.M., M.N., A.E., P.S., M.A.E. and R.T.F.; supervision, M.N., A.E., C.W.S., W.A., P.S., S.C., M.A.E and R.T.F. All authors have read and agreed to the published version of the manuscript.

## Funding

This research was funded by the Egyptian Government missions sector PhD scholarship awarded to A.Y.M. and was supported by the self-funded PhD project for A.A.

## Declaration of competing interest

The authors declare that they have no known competing financial interests or personal relationships that could have appeared to influence the work reported in this paper.

## Data availability

Data will be made available on request.

## Acknowledgments

Authors would like to thank the University of Leicester Core Biotechnology Services Electron Microscopy Facility, for the use of their Transmission Electron Microscope. Authors would also like to thank Dr Abdullah Isreb, Dr Sim Singhrao and Dr Sarah Dennison from University of Central Lancashire (UCLan), as well as Abdulwahhab Khedr and Mohamed Soliman from De Montfort University for their support and scientific discussions. Authors are grateful to Dr Julie Burrows and Dr Antony Ashton from UCLan for training A.A. on the basics of in vitro cell culture techniques and bioassays used in this work. Authors would like to thank Dr Gail Welsby for providing A.A. training for the use of the fluorescence microscope. Thanks to the technical staff in JB Firth analytical suite at UCLan for their assistance and training of A.A. on some of the analytical techniques used in this work. Authors are grateful to Dr Philip Welsby for providing the aspirin used in this project as in-kind contribution.

## Appendix A. Supplementary data

Supplementary data to this article can be found online at https://doi.org/10.1016/j.jddst.2022.104052.

## References

[1] I.I. Ship, Epidemiologic aspects of recurrent aphthous ulcerations, Oral Surg. Oral Med. Oral Pathol. 33 (1972) 400–406, https://doi.org/10.1016/0030-4220(72)90469-0.
[2] J. Bell, Amlexanox for the treatment of recurrent aphthous ulcers, Clin. Drug Invest. (2005), https://doi.org/10.2165/00044011-200525090-00001.
[3] W.C. Gonsalves, A.C. Chi, B.W. Neville, Common Oral Lesions: Part I. Superficial Mucosal Lesions, American Family Physician, 2007.
[4] M. Okada, H. Itoh, T. Hatakeyama, H. Tokumitsu, R. Kobayashi, Hsp90 is a direct target of the anti-allergic drugs disodium cromoglycate and amlexanox, Biochem. J. 374 (2003) 433–441, https://doi.org/10.1042/BJ20030351.

[5] S.G. Rani, S.K. Mohan, C. Yu, Molecular level Interactions of S100A13 with amlexanox: inhibitor for formation of the multiprotein complex in the nonclassical pathway of acidic fibroblast growth factor, Biochemistry 49 (2010) 2585–2592, https://doi.org/10.1021/bi9019077.

[6] Shannon M. Reilly, S.H. Chiang, S.J. Decker, L. Chang, M. Uhm, M.J. Larsen, J. R. Rubin, J. Mowers, N.M. White, I. Hochberg, M. Downes, R.T. Yu, C. Liddle, R. M. Evans, D. Oh, P. Li, J.M. Olefsky, A.R. Saltiel, An inhibitor of the protein kinases TBK1 and IKK-ε improves obesity-related metabolic dysfunctions in mice, Nat. Med. 19 (2013) 313–321, https://doi.org/10.1038/nm.3082.

[7] D.D. Darshan, C.N.V. Kumar, A.D.M. Kumar, N.S. Manikantan, D. Balakrishnan, M. P. Uthkal, Clinical study to know the efficacy of Amlexanox 5% with other topical Antiseptic, Analgesic and Anesthetic agents in treating minor RAS, J. Int. Oral Health : JIOH 6 (2014) 5–11.

[8] B. Murray, N. McGuinness, P. Biagioni, P. Hyland, P.J. Lamey, A comparative study of the efficacy of AphthealTM in the management of recurrent minor aphthous ulceration, J. Oral Pathol. Med. 34 (2005) 413–419, https://doi.org/10.1111/J.1600-0714.2005.00334.X.

[9] J. Bailey, C. Mccarthy, P.C. Smith, Clinical inquiry. What is the most effective way to treat recurrent canker sores? J. Fam. Pract. 60 (10) (2011) 621–632.

[10] N.R. Edgar, D. Saleh, R.A. Miller, Recurrent aphthous stomatitis: a review, J. Clin. Aesthetic Dermatol. 10 (3) (2017) 26–36.

[11] L. Preeti, K.T. Magesh, K. Rajkumar, R. Karthik, Recurrent aphthous stomatitis, J. Oral Maxillofac. Pathol. (2011), https://doi.org/10.4103/0973-029X.86669.

[12] V. Hearnden, V. Sankar, K. Hull, D.V. Juras, M. Greenberg, A.R. Kerr, P. B. Lockhart, L.L. Patton, S. Porter, M.H. Thornhill, New developments and opportunities in oral mucosal drug delivery for local and systemic disease, Adv. Drug Deliv. Rev. 64 (2012) 16–28, https://doi.org/10.1016/J.ADDR.2011.02.008.

[13] J. Yang, A. Bahreman, G. Daudey, J. Bussmann, R.C.L. Olsthoorn, A. Kros, Drug delivery via cell membrane fusion using lipopeptide modified liposomes, ACS Cent. Sci. 2 (2016) 621–630, https://doi.org/10.1021/ACSCENTSCI.6B00172.

[14] M. Trif, O. Craciunescu, Liposome as efficient system for intracellular delivery of bioactive molecules, in: Nanotechnology and Functional Foods, John Wiley & Sons, Ltd, Chichester, UK, 2015, pp. 191–213, https://doi.org/10.1002/9781118462157.ch12.

[15] Y. Chen, X. Feng, S. Meng, Site-specific drug delivery in the skin for the localized treatment of skin diseases, Expet Opin. Drug Deliv. (2019), https://doi.org/10.1080/17425247.2019.1645119.

[16] S. Hua, E. Marks, J.J. Schneider, S. Keely, Advances in oral nano-delivery systems for colon targeted drug delivery in inflammatory bowel disease: selective targeting to diseased versus healthy tissue, Nanomed. Nanotechnol. Biol. Med. (2015), https://doi.org/10.1016/j.nano.2015.02.018.

[17] C. Kelly, C. Jefferies, S.C.-J. delivery, Of drug, 2011, undefined, 2011. Targeted liposomal drug delivery to monocytes and macrophages, downloads.hindawi.com, 11, https://doi.org/10.1155/2011/727241, 2011.

[18] K.D. Fugit, B.D. Anderson, Dynamic, nonsink method for the simultaneous determination of drug permeability and binding coefficients in liposomes, Mol. Pharm. 11 (2014) 1314–1325, https://doi.org/10.1021/MP400765N.

[19] K.D. Fugit, B.D. Anderson, The role of pH and ring-opening hydrolysis kinetics on liposomal release of topotecan, J. Contr. Release 174 (2014) 88–97, https://doi.org/10.1016/J.JCONREL.2013.11.003.

[20] S.S. Marques, I.I. Ramos, S.R. Fernandes, L. Barreiros, S.A.C. Lima, S. Reis, M.R. M. Domingues, M.A. Segundo, Insights on ultrafiltration-based separation for the purification and quantification of methotrexate in nanocarriers, Molecules 25 (2020), https://doi.org/10.3390/MOLECULES25081879.

[21] Y. Nagasaka, F. Ishii, Interaction between erythrocytes from three different animals and emulsions prepared with various lecithins and oils, Colloids Surf. B Biointerfaces 22 (2001) 141–147, https://doi.org/10.1016/S0927-7765(01)00148-5.

[22] A.M.A. Elhissi, M.A.A. O'Neill, S.A. Roberts, K.M.G. Taylor, A calorimetric study of dimyristoylphosphatidylcholine phase transitions and steroid-liposome interactions for liposomes prepared by thin film and proliposome methods, Int. J. Pharm. 320 (2006) 124–130, https://doi.org/10.1016/j.ijpharm.2006.04.015.

[23] A. Elhissi, K. Hidayat, D.A. Phoenix, E. Mwesigwa, S. Crean, W. Ahmed, A. Faheem, K.M.G. Taylor, Air-jet and vibrating-mesh nebulization of niosomes generated using a particulate-based proniosome technology, Int. J. Pharm. 444 (2013) 193–199, https://doi.org/10.1016/j.ijpharm.2012.12.040.

[24] G. Bozzuto, A. Molinari, CEOR-52063-c-quality–cost-and-quality-of-life-pharmacoeconomic-analysi, Int. J. Nanomed. Dovepress 10 (2015) 975–999, https://doi.org/10.2147/IJN.S68861.

[25] W. Chanput, J.J. Mes, H.J. Wichers, THP-1 cell line: an in vitro cell model for immune modulation approach, Int. Immunopharm. (2014), https://doi.org/10.1016/j.intimp.2014.08.002.

[26] Z. Qin, The Use of THP-1 Cells as a Model for Mimicking the Function and Regulation of Monocytes and Macrophages in the Vasculature, 2012, https://doi.org/10.1016/j.atherosclerosis.2011.09.003. Atherosclerosis.

[27] M. Daigneault, J.A. Preston, H.M. Marriott, M.K.B. Whyte, D.H. Dockrell, The identification of markers of macrophage differentiation in PMA-stimulated THP-1 cells and monocyte-derived macrophages, PLoS One 5 (2010), https://doi.org/10.1371/JOURNAL.PONE.0008668.

[28] M.B. Maeß, B. Wittig, A. Cignarella, S. Lorkowski, Reduced PMA enhances the responsiveness of transfected THP-1 macrophages to polarizing stimuli, J. Immunol. Methods 402 (2014) 76–81, https://doi.org/10.1016/j.jim.2013.11.006.

[29] E. Pedraza-Brindis, C. K.S.-R, Culture Supernatants of Cervical Cancer Cells Induce an M2 Phenotypic Profile in THP-1 Macrophages, Elsevier, 2016, https://doi.org/10.1016/j.cellimm.2016.07.001 undefined, 2016.

[30] W. Chanput, J.J. Mes, H.F.J. Savelkoul, H.J. Wichers, Characterization of polarized THP-1 macrophages and polarizing ability of LPS and food compounds, Food Funct. 4 (2013) 266–276, https://doi.org/10.1039/c2fo30156c.

[31] G. Lopez-Castejon, D. Brough, Understanding the mechanism of IL-1β secretion, Cytokine Growth Factor Rev. (2011), https://doi.org/10.1016/j.cytogfr.2011.10.001.

[32] F.O. Martinez, S. Gordon, M. Locati, A. Mantovani, Transcriptional profiling of the human monocyte-to-macrophage differentiation and polarization: new molecules and patterns of gene expression, J. Immunol. 177 (2006) 7303–7311, https://doi.org/10.4049/jimmunol.177.10.7303.

[33] F. Meng, C.A. Lowell, Lipopolysaccharide (LPS)-induced macrophage activation and signal transduction in the absence of Src-family kinases Hck, Fgr, and Lyn, J. Exp. Med. 185 (1997) 1661–1670, https://doi.org/10.1084/jem.185.9.1661.

[34] E. Müller, P.F. Christopoulos, S. Halder, A. Lunde, K. Beraki, M. Speth, I. Øynebråten, A. Corthay, Toll-like receptor ligands and interferon-γ synergize for induction of antitumor M1 macrophages, Front. Immunol. 8 (2017), https://doi.org/10.3389/FIMMU.2017.01383/FULL.

[35] H. Shi, Y. Guo, Y. Liu, B. Shi, X. Guo, L. Jin, S. Yan, The in vitro effect of lipopolysaccharide on proliferation, inflammatory factors and antioxidant enzyme activity in bovine mammary epithelial cells, Anim. Nutr. 2 (2016) 99–104, https://doi.org/10.1016/j.aninu.2016.03.005.

[36] C. Xie, C. Liu, B. Wu, Y. Lin, T. Ma, H. Xiong, Q. Wang, Z. Li, C. Ma, Z. Tu, Effects of IRF1 and IFN-interaction on the M1 polarization of macrophages and its antitumor function, Int. J. Mol. Med. 38 (2016) 148–160, https://doi.org/10.3892/ijmm.2016.2583.

[37] N. Parameswaran, S. Patial, Tumor necrosis factor-α signaling in macrophages, Crit. Rev. Eukaryot. Gene Expr. 20 (2010) 87–103, https://doi.org/10.1615/CRITREVEUKARGENEEXPR.V20.I2.10.

[38] I. Belenguer-Guallar, Y. Jiménez-Soriano, A. Claramunt-Lozano, Treatment of recurrent aphthous stomatitis. A literature review, J. Clin. Exper. Dent. 6 (2014) e168, https://doi.org/10.4317/JCED.51401.

[39] Yitong Liu, S. Fang, X. Li, J. Feng, J. Du, L. Guo, Y. Su, J. Zhou, G. Ding, Y. Bai, S. Wang, H. Wang, Yi Liu, Aspirin inhibits LPS-induced macrophage activation via the NF-κB pathway, Sci. Rep. 7 (1 7) (2017) 1–11, https://doi.org/10.1038/s41598-017-10720-4, 2017.

[40] I. Treede, A. Braun, P. Jeliaskova, T. Giese, J. Füllekrug, G. Griffiths, W. Stremmel, R. Ehehalt, TNF-α-induced up-regulation of pro-inflammatory cytokines is reduced by phosphatidylcholine in intestinal epithelial cells, BMC Gastroenterol. 9 (2009), https://doi.org/10.1186/1471-230X-9-53.

[41] I. Treede, A. Braun, R. Sparla, M. Kühnel, T. Giese, J.R. Turner, E. Anes, H. Kulaksiz, J. Füllekrug, W. Stremmel, G. Griffiths, R. Ehehalt, Anti-inflammatory effects of phosphatidylcholine, J. Biol. Chem. 282 (2007) 27155–27164, https://doi.org/10.1074/JBC.M704408200.

[42] M. Chen, H. Pan, Y. Dai, J. Zhang, Y. Tong, Y. Huang, M. Wang, H. Huang, Phosphatidylcholine regulates NF-κB activation in attenuation of LPS-induced inflammation: evidence from in vitro study. https://doi.org/10.1080/19768354.2017.1405072 22, 7–14, 2017. https://doi.org/10.1080/19768354.2017.1405072.

[43] S. Hobbs, M. Reynoso, P. A.G., in: Undefined, 2018. LPS-stimulated NF-κB P65 Dynamic Response Marks the Initiation of TNF Expression and Transition to IL-10 Expression in RAW 264.7 Macrophages, Wiley Online Library, 2018, https://doi.org/10.14814/phy2.13914, 6.

[44] T.M. Allen, G.A. Austin, A. Chonn, L. Lin, K.C. Lee, Uptake of liposomes by cultured mouse bone marrow macrophages: influence of liposome composition and size, Biochim. Biophys. Acta Biomembr. 1061 (1991) 56–64, https://doi.org/10.1016/0005-2736(91)90268-D.

[45] V. Komalla, V.S.R.R. Allam, P.C.L. Kwok, B. Sheikholeslami, L. Owen, A. Jaffe, S. A. Waters, S. Mohammad, B.G. Oliver, H. Chen, M. Haghi, A phospholipid-based formulation for the treatment of airway inflammation in chronic respiratory diseases, Eur. J. Pharm. Biopharm. 157 (2020) 47–58, https://doi.org/10.1016/J.EJPB.2020.09.017.